

## Supplementary Materials for

### **Antiarrhythmics cure brain arrhythmia: The imperativeness of subthalamic ERG K<sup>+</sup> channels in parkinsonian discharges**

Chen-Syuan Huang, Guan-Hsun Wang, Chun-Hwei Tai, Chun-Chang Hu, Ya-Chin Yang

Published 10 May 2017, *Sci. Adv.* **3**, e1602272 (2017)

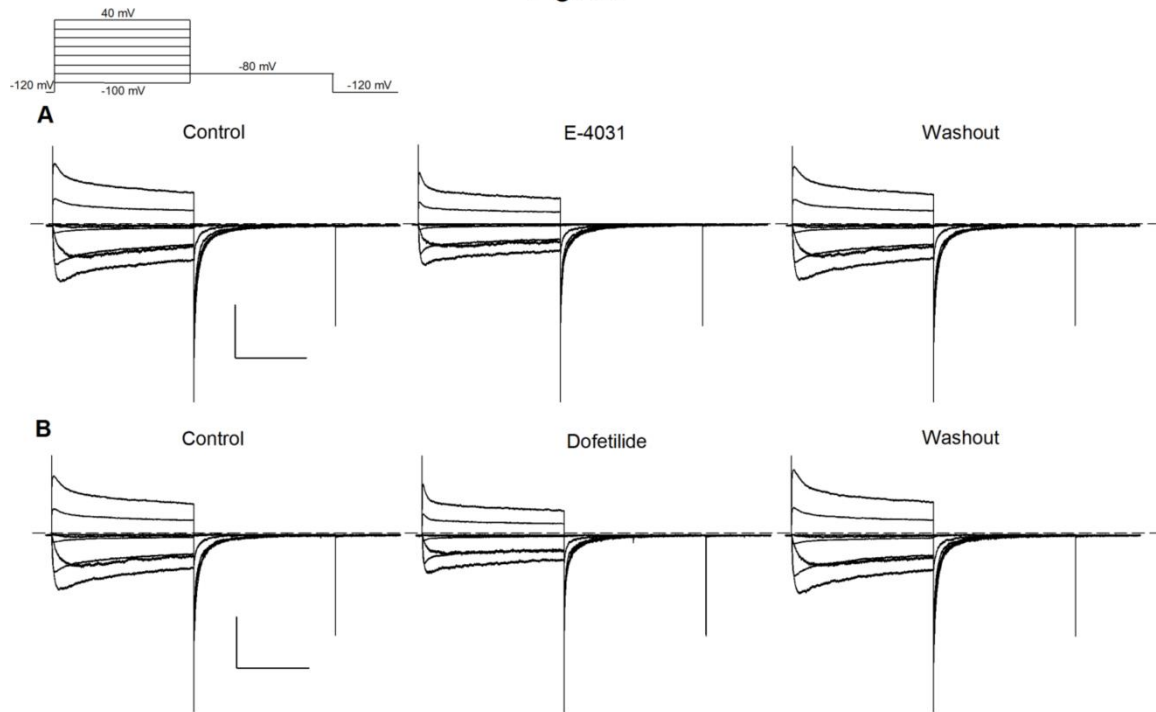
DOI: 10.1126/sciadv.1602272

#### **This PDF file includes:**

- fig. S1. The original currents of Fig. 1.
- fig. S2. Characterization of ERG K<sup>+</sup> currents by channel activator PD-118057 in acutely dissociated subthalamic neurons following similar experimental protocols and analyses of Fig. 1.
- fig. S3. The effect of PD-118057 on E-4031-sensitive currents.
- fig. S4. The effect of the ERG inhibitor and activator on spontaneous firing of subthalamic neurons in acute STN slices from parkinsonian rats.
- fig. S5. The distinct effects of the ERG inhibitor dofetilide on a pair of simultaneously recorded neurons, with one firing in the spontaneous tonic mode and the other in the burst mode.
- fig. S6. The effect of ERG channel inhibitor and activator on burst discharges in rat STN slices.
- fig. S7. The effect of ERG channel inhibitor and activator on the spontaneous firing activity of subthalamic neurons at low and high temperatures.
- fig. S8. Continuous recording of spontaneous firing activity in acute STN slices before, during, and after application of 5- $\mu$ M E-4031 (A) or 0.5- $\mu$ M PD-118057 (B).
- fig. S9. The effect of ERG channel inhibitor and activator on the plateau depolarization in the presence of tetrodotoxin.
- fig. S10. The effect of ERG channel modulation on rearing scores and the asymmetric limb use.
- fig. S11. Inhibition of ERG channels ameliorates abnormal burst discharges in parkinsonian rats.
- Methods for figs. S10 (E and F) and S11
- References (100, 101)

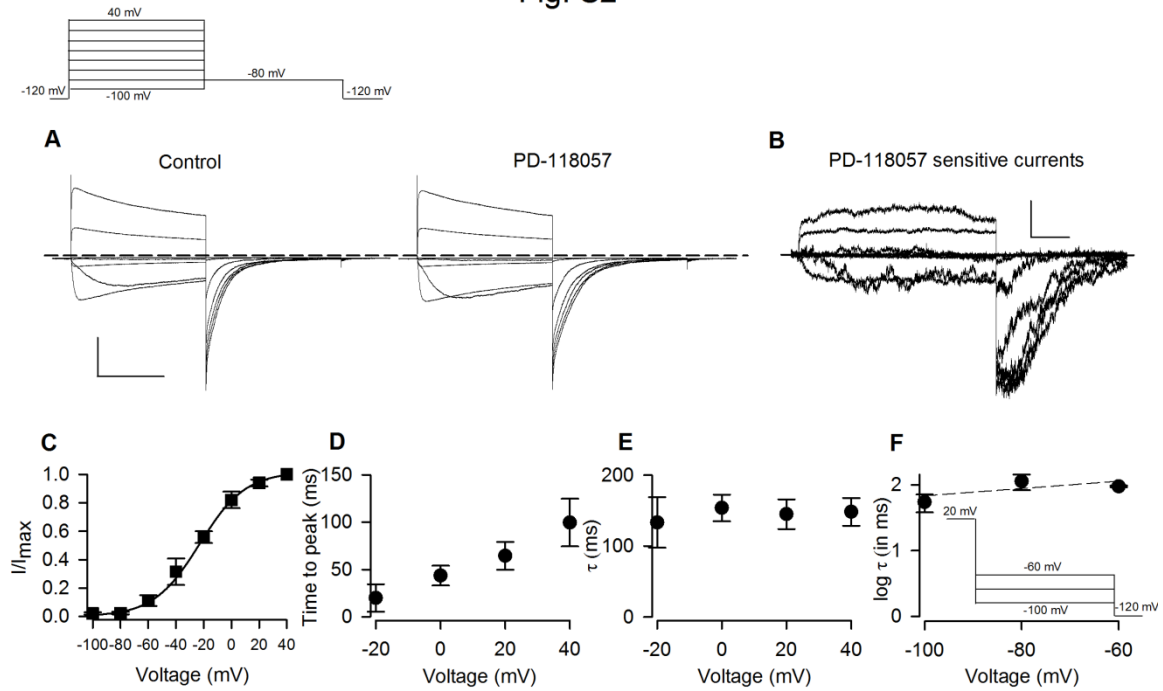
# Supplementary Materials

Fig. S1



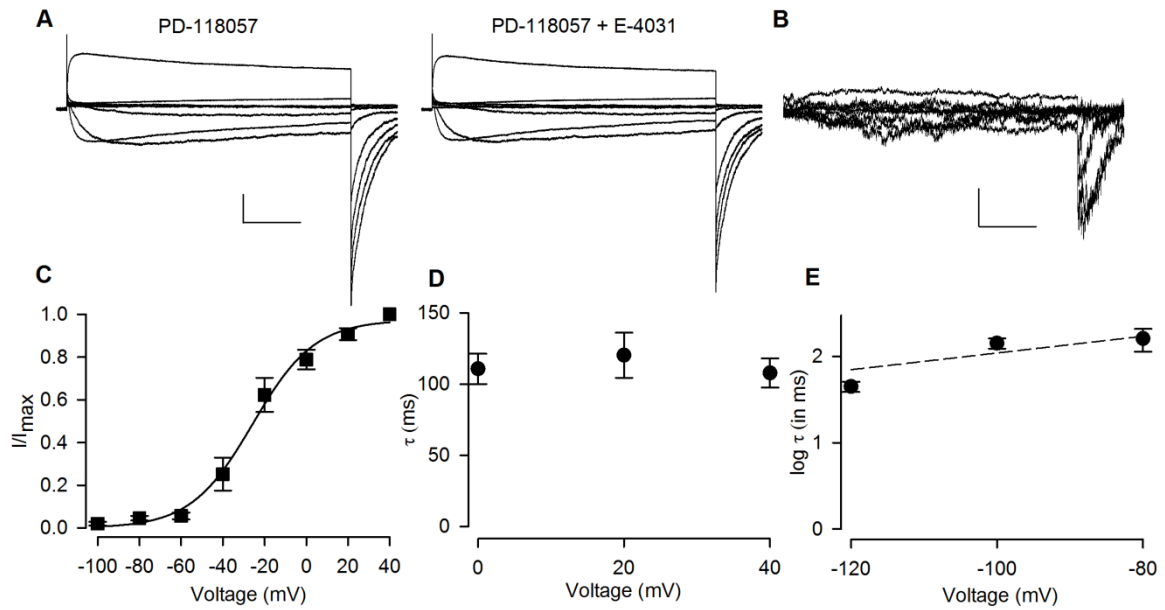
**fig. S1. The original currents of Fig. 1.** The original currents recorded before, during, and after application of 600 nM E-4031 (**A**) or 100 nM dofetilide (**B**). The difference between the currents in (**A**) and (**B**) yields E-4031- and dofetilide-sensitive currents shown in Fig. 1A and 1B, respectively. Scale bars: 2 nA/500 ms. Animals used: a p12 rat.

Fig. S2



**fig. S2. Characterization of ERG K<sup>+</sup> currents by channel activator PD-118057 in acutely dissociated subthalamic neurons following similar experimental protocols and analyses of Fig. 1.** (A) The original currents recorded in the absence (left) and presence (right) of 1 μM PD-118057. Scale bars: 1 nA/500 ms. (B) The difference between the currents in (A) yields PD-118057-sensitive currents with characteristic hook tails upon repolarization. Scale bars: 200 pA/200 ms. (C) Normalized peak tail PD-118057-sensitive currents ( $I/I_{max}$ ) are plotted against voltages ( $V_t$ ) of the preceding depolarization and fitted with a Boltzmann function ( $I/I_{max}=1/(1+\exp([V_{0.5}-V_t]/k))$ ) with  $V_{0.5}$  of -24 mV and  $k$  of 16 (n=6). (D) The degree of inactivation is dependent on the depolarizing potential. Following a prepulse depolarization from -20 mV to 40 mV, the time to peak of the PD-118057-sensitive tail current elicited by the subsequent repolarization at -80 mV is measured and plotted against the prepulse voltage (n=6). (E) The time constant ( $\tau$ ) of the tail current decay at -80 mV is independent of the prepulse voltage between -20 mV and 40 mV (n=6). (F) The logarithm of the decaying time constants is plotted against the repolarization potential and fitted with a linear function  $y=2.39+0.01x$  (n=7). Animals used: p9-15 rats.

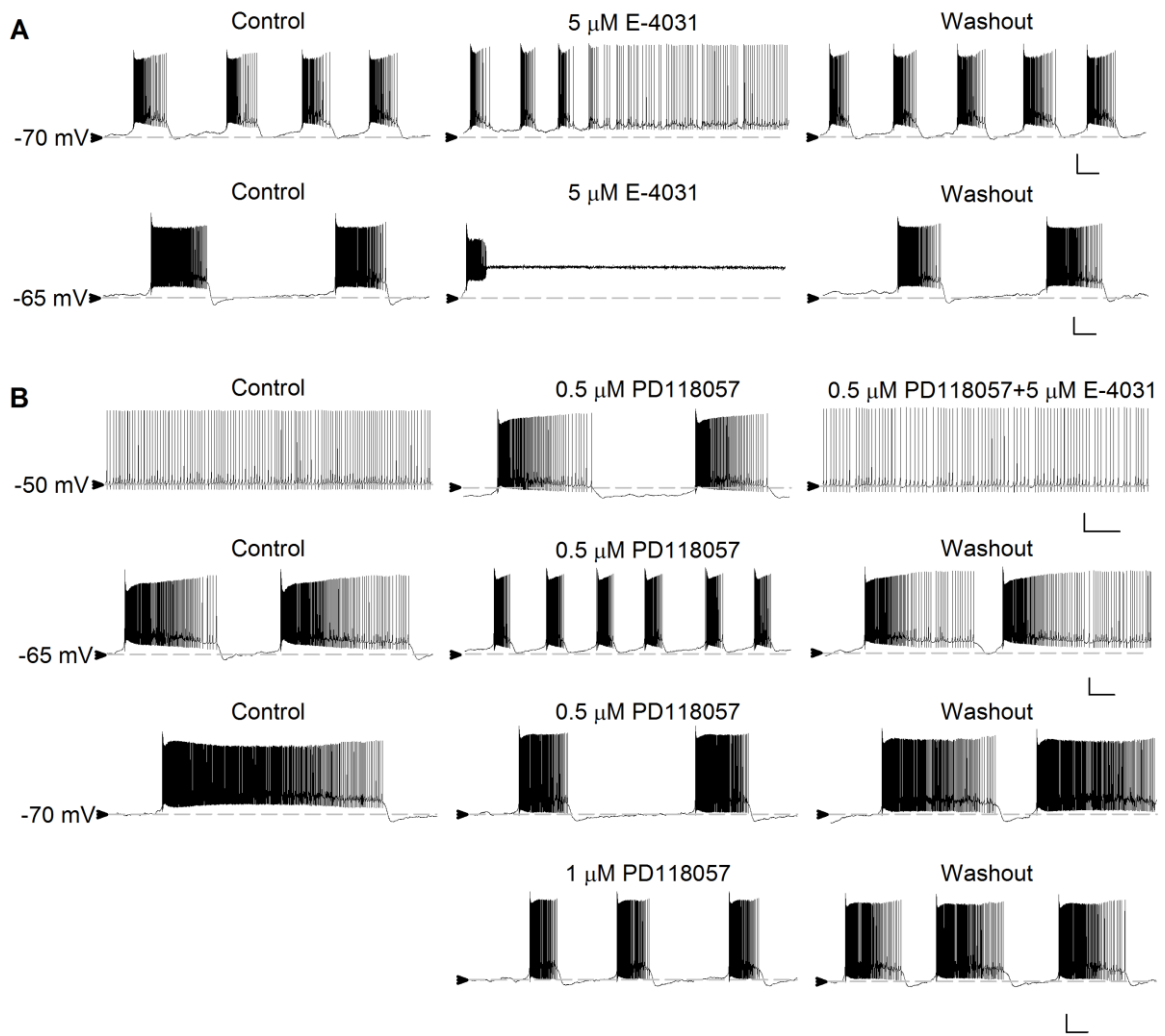
Fig. S3



**fig. S3. The effect of PD-118057 on E-4031-sensitive currents.** Experimental protocols and analyses are similar to those of Fig.1, except that E-4031 (600 nM)-sensitive currents are obtained in the presence of PD-118057 (1  $\mu$ M). **(A)** The original currents recorded in the presence of 1  $\mu$ M PD-118057 with (right) and without (left) 600 nM E-4031. Scale bar: 1 nA/200 ms. **(B)** The difference between the currents in (A) yields E-4031-sensitive currents in the presence of PD-118057. The subtracted currents display characteristic large tail currents upon repolarization. Scale bars: 200 pA/200 ms. **(C)** The normalized peak tail current is plotted against the voltage of the preceding depolarization and fitted with a Boltzmann function with a  $V_{0.5}$  of -29 mV and a slope factor of 14 ( $n=6$ ). **(D)** The decay time constant ( $\tau$ ) is independent of the preceding depolarization ( $n=6$ ). **(E)** The decay of tail current is fitted with a mono-exponential function. The logarithm of the decay time constant is plotted against the repolarization potential and fitted with a linear function  $y=3.01+0.01x$  ( $n=3$ ). Animals used: p9-15 rats

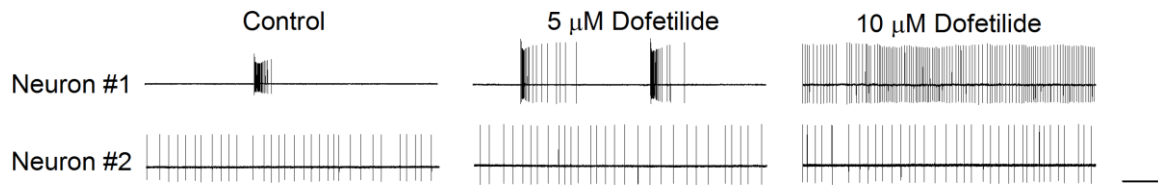
Fig. S4

PD rats



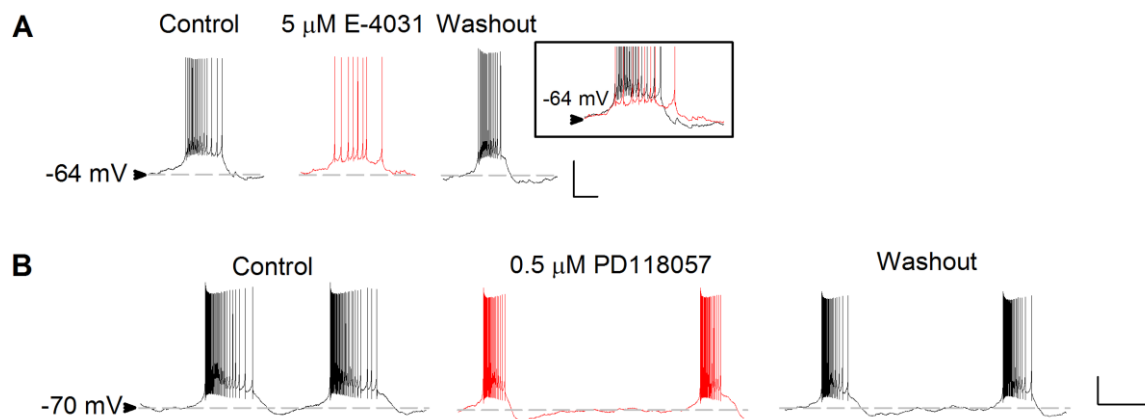
**fig. S4. The effect of the ERG inhibitor and activator on spontaneous firing of subthalamic neurons in acute STN slices from parkinsonian rats.** (A) Two representative neurons that display spontaneous bursts with longer plateau compared to the cases in normal animals are shown (Also see Fig. 6A, middle panels). Upon application of 5  $\mu$ M E-4031, one neuron is switched from bursts into spikes (upper panel) and the other is silenced (lower panel). (B) *Upper panel*, A representative neuron displays spontaneous spikes with a baseline membrane potential of  $\sim$ -50 mV. 0.5  $\mu$ M PD-118057 hyperpolarizes the membrane and converts the discharge mode from tonic spike into burst, an effect readily abolished by co-application of 5  $\mu$ M E-4031. *Middle panel*, 0.5  $\mu$ M PD-118057 evidently hyperpolarizes the burst plateau and also shortens the burst duration. *Lower panel*, Another neuron displays spontaneous bursts with even longer plateaus ( $\sim$ 20 s). Again, PD-118057 hyperpolarizes the burst plateau and shortens the burst duration in a dose-dependent manner. Scale bars: 20 mV/2s. Animals used: p32-46 parkinsonian (PD) rats.

Fig. S5



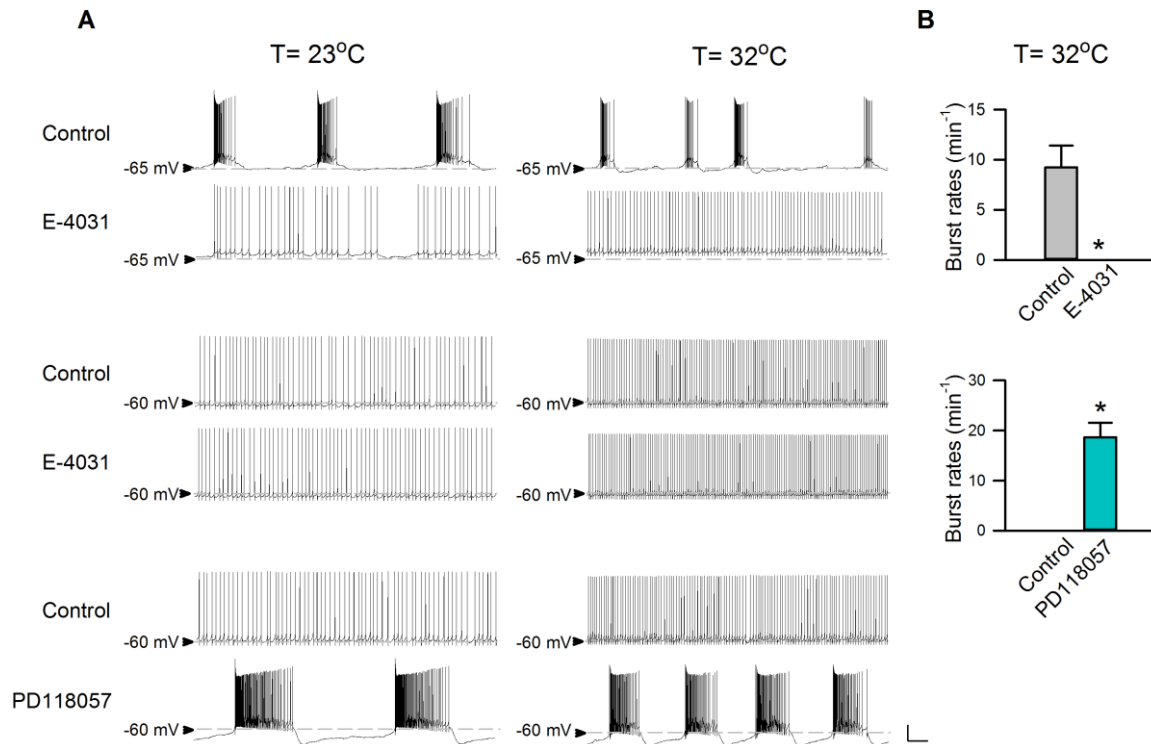
**fig. S5. The distinct effects of the ERG inhibitor dofetilide on a pair of simultaneously recorded neurons with one firing in the spontaneous tonic mode and the other in the burst mode.** Extracellular pair recording of spontaneous discharges of neurons is performed in a STN slice. Application of 5-10  $\mu\text{M}$  dofetilide shifts the firing pattern to the tonic mode in the originally bursting neuron (Neuron #1) but has no significant effect in the neuron firing in the tonic mode (Neuron #2). Scale bar: 2 s. Animal used: a p22 mouse.

Fig. S6



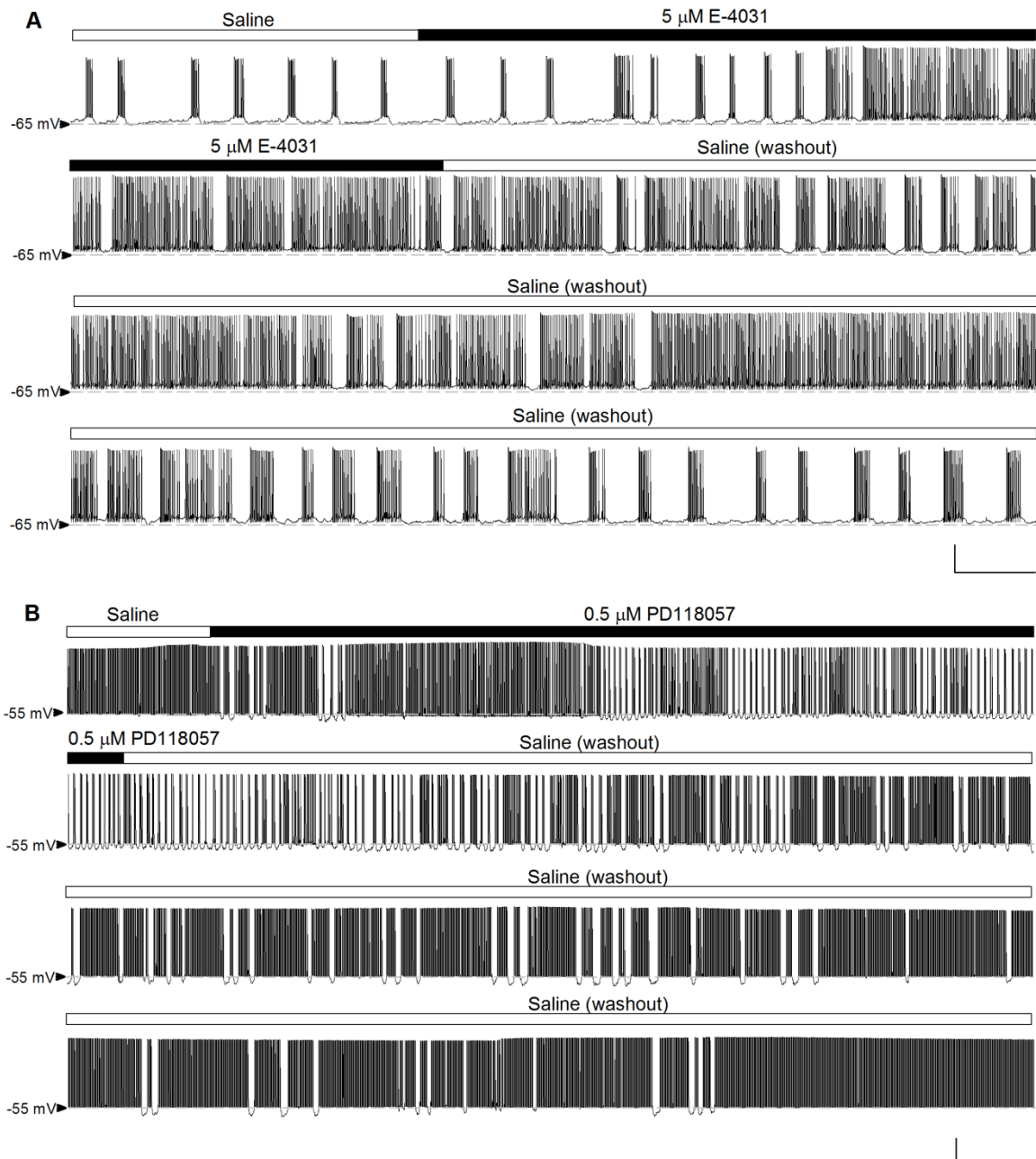
**fig. S6. The effect of ERG channel inhibitor and activator on burst discharges in rat STN slices.** (A) In a representative rat subthalamic neuron, E-4031 (5  $\mu\text{M}$ ) reduces burst discharges. *Inset*, Superimposed bursts in the absence (black) and the presence (red) of 5  $\mu\text{M}$  E-4031 demonstrate a decreased afterhyperpolarization by E-4031. Scale bars: 20 mV/1 s. (B) In a rat subthalamic neuron that spontaneously fires in bursts with relatively long plateau, 0.5  $\mu\text{M}$  PD-118057 shortens burst duration. Scale bars: 20 mV/2 s. Animals used: p30 and p23 rats for A and B, respectively.

Fig. S7



**fig. S7. The effect of ERG channel inhibitor and activator on the spontaneous firing activity of subthalamic neurons at low and high temperatures.** (A) A representative subthalamic neuron that spontaneously fires in bursts and in tonic spikes at baseline membrane potential of  $\sim$ -65 and -60 mV, respectively, was recorded at either room temperature (23°C, left column) or 32°C (right column). 5  $\mu$ M E-4031 abolishes bursts but does not significantly alters tonic discharges at both temperatures. On the other hand, 0.5  $\mu$ M PD-118057 readily turns tonic spikes into bursts at both temperatures. Scale bars: 20 mV/1s. (B) The effects of 5  $\mu$ M E-4031 (n=4) and 0.5  $\mu$ M PD-118057 (n=3) on burst rates at 32°C are analyzed. \*p<0.05 compared to control by paired two-tailed Student's *t* test. Animals used: p22-27 rats.

Fig. S8

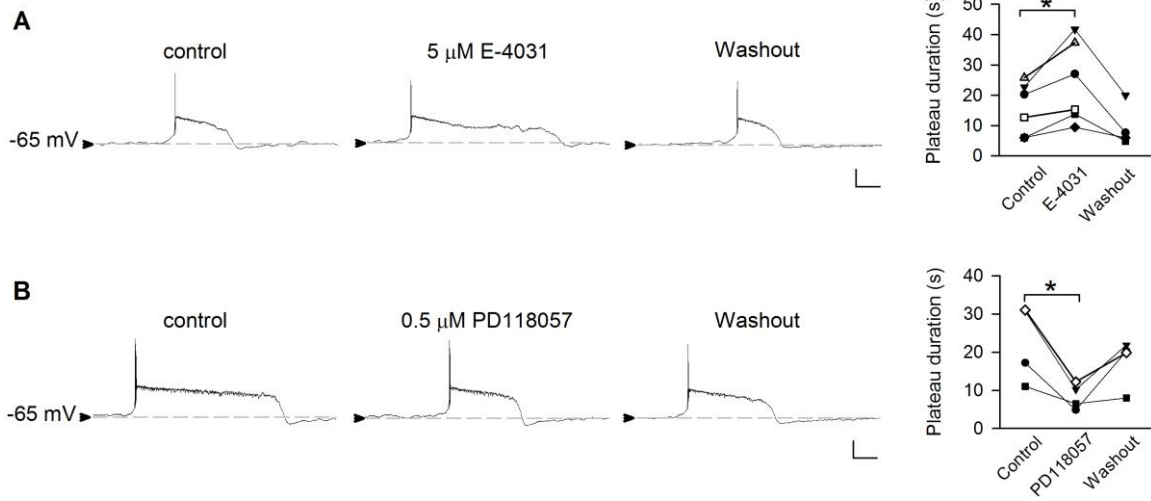


**fig. S8. Continuous recording of spontaneous firing activity in acute STN slices before, during, and after application of 5  $\mu\text{M}$  E-4031 (A) or 0.5  $\mu\text{M}$  PD-118057 (B). The whole-cell current-clamp recording is done on a representative subthalamic neuron from a p23 mouse (A) or from a p40 rat (B). Scale bars: 40 mV/0.5 min.**



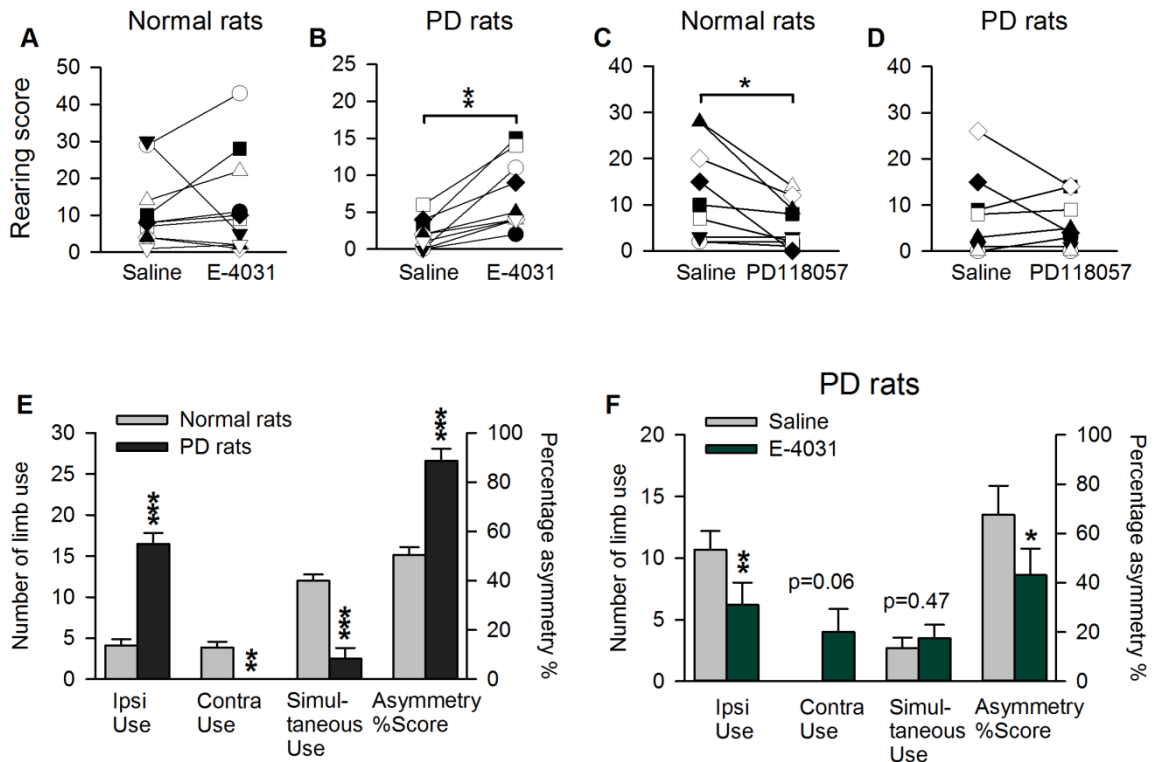
Fig. S9

In the presence of 100 nM TTX



**fig. S9. The effect of ERG channel inhibitor and activator on the plateau depolarization in the presence of tetrodotoxin.** Spontaneous plateau depolarization is isolated by 100 nM tetrodotoxin (TTX). 5  $\mu$ M E-4031 (**A**, n=6) significantly prolongs, while 0.5  $\mu$ M PD-118057 (**B**, n=4) markedly shortens the plateau duration. Different symbols denote different neurons (the hollow ones are neurons from parkinsonian or PD rats). Measurements from the same neuron are connected by solid lines. Animals used: p22-28 normal rats and p32-33 PD rats. Scale bars: 20 mV/2 s.

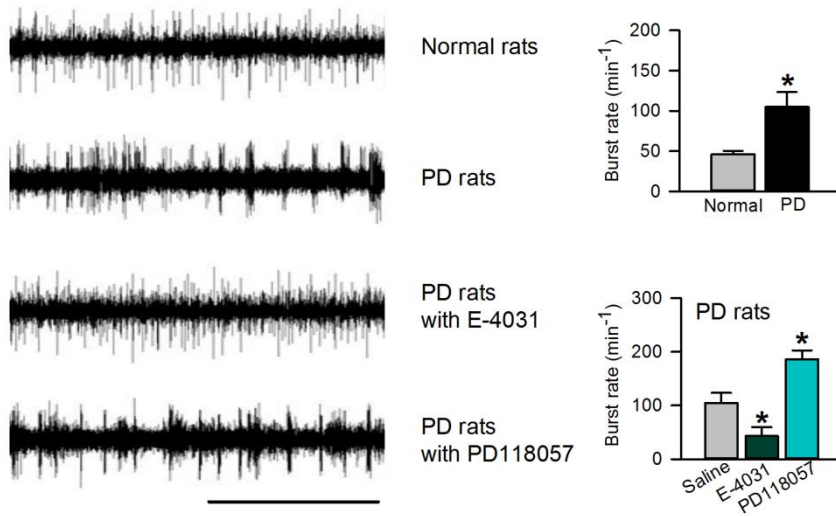
Fig.S10



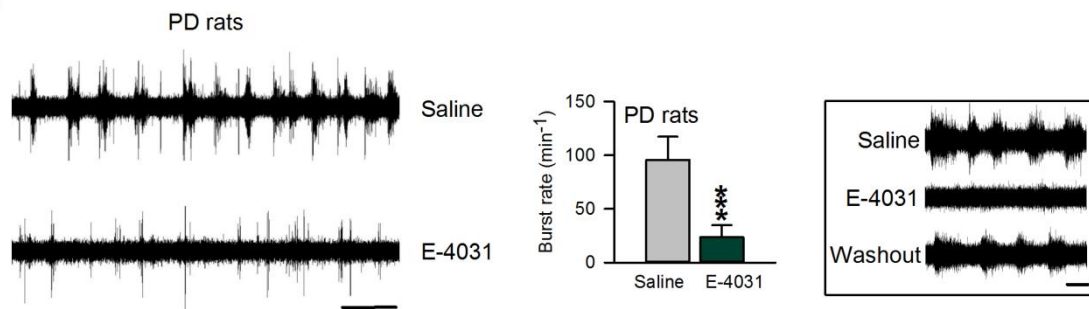
**fig. S10. The effect of ERG channel modulation on rearing scores and the asymmetric limb use.** (A)-(D) The original data of rearing scores documented for microinjection of E-4031 (200  $\mu$ M, n=10 for both normal and parkinsonian or PD groups) or PD-118057 (200  $\mu$ M, n=9 for both normal and PD groups) are compared with those injected with normal saline (before drug) within the same group. The different symbols denote different animals, and measurements from the same animal are connected by solid lines. There is a clear trend that E-4031 (B, n=10) increases the rearing score in the PD group, while PD-118057 (C, n=9) renders normal rats hypokinetic (\* $p$ <0.05; \*\* $p$ <0.01 by paired two-tailed Student's  $t$  test). (E)-(F) Experimental methods and analyses follow those developed by the Schallert's group (60,61; see Methods below). The motor impairment characterized by the number of ipsilateral (Ipsi), contralateral (Contra) and simultaneous limb use events (the left vertical axis) and the corresponding asymmetry scores (the right vertical axis) in the cylinder test in the PD rats are recovered by microinjection of 200  $\mu$ M of E-4031 (E, n=10 and 4 for normal and PD rats without microinjection, respectively; \*\* $p$ <0.01; \*\*\* $p$ <0.001 by unpaired two-tailed Student's  $t$  test; F, n=10 for microinjection of saline and then E-4031 into PD rats; \* $p$ <0.05; \*\* $p$ <0.01 by paired two-tailed Student's  $t$  test). Animals used: 2-3 month rats (weighing 260-380 g).

Fig. S11

A



B



**fig. S11. Inhibition of ERG channels ameliorates abnormal burst discharges in parkinsonian rats.** (A) Experimental methods and analyses follow those described in (10) (see Methods below). *Left panels*, Typical in vivo extracellular recordings of subthalamic (STN) discharges in normal and parkinsonian (PD, with 6-OHDA lesion) rats, which further receive either E-4031 or PD-118057 are shown. *Right panels*, The burst rate in PD rats is significantly higher than that in normal rats ( $n=6$  and  $10$  for normal and PD rats, respectively;  $*p<0.05$  by unpaired two-tailed Student's  $t$  test). Microinjection of E-4031 ( $200 \mu\text{M}$ ) significantly reduces the burst rate in PD rats, whereas injection of PD-118057 ( $200 \mu\text{M}$ ) exacerbates the abnormal burst discharges ( $n=10, 6,$  and  $4$  for saline, E-4031, and PD-118057, respectively;  $*p<0.05$  by one-way ANOVA with the Holm-Šidák multiple comparison test). (B) The experimental methods and analyses are similar to part A except that the tungsten electrodes for recording and the microdialysis cannula for drug application are used (see Methods). The microdialysis probe membrane ensures more constant extent as well as concentration of drug delivery and more effective washout. Continuous infusion of  $2 \text{ mM}$  (and thus  $\sim 200 \mu\text{M}$  outside the probe membrane, see Methods) of E-4031 through the microdialysis probe evidently and reversibly (see *box*) reduces bursts in STN ( $n=7$ ;  $***p<0.001$  by paired two-tailed Student's  $t$  test). Scale bars:  $1 \text{ s}$ . Animals used: 2-3 month rats (weighing  $260\text{-}380 \text{ g}$ ).

## Methods for fig. S10, E and F, and fig. S11

### *The cylinder test*

A modified version (59) of the cylinder test developed originally by Schallert's group (60, 61) was used to assess limb-use asymmetry. Briefly, the rats were placed in a clear cylinder (30 cm tall by 18 cm diameter) to record movement of the forelimbs by which they make wall contact during a full rear. The numbers of wall contacts using the unaffected (ipsilateral), affected (contralateral) and both (simultaneous) forelimbs are recorded in specified sessions, and used to calculate the asymmetry score, which is defined as the number of ipsilateral limb usage plus  $\frac{1}{2}$  the number of simultaneous limb usage, divided by the total number of observations. In this asymmetry test, the higher score would signal greater reliance on the intact limb, and vice versa. For assessment of the effect of ERG inhibitor on limb use performance, the cylinder test follows immediately after microinjection of pharmacological agents. On each session a maximum of 20 limb uses in 5 minutes were recorded.

### *In vivo electrophysiological recording*

In vivo electrophysiological recordings were done with the methods described before (10). Briefly, the skull and dura mater were removed from an anesthetized male Wistar rat (weighing 260-380g). A metal micro-injection cannula was placed into STN according to the stereotaxic coordinate (AP – 3.8 mm, L 2.4 mm, D 7.5 mm from bregma) at a 20 degrees angle from vertical line on sagittal plan. The cannula was then connected by a polyethylene catheter to a Hamilton microsyringe driven by an infusion pump (Harvard Apparatus, UK). For quasi-single unit recordings, a bundle of 4 insulated stainless steel electrodes (0.002 inch in diameter, no. 304; California Fine Wire) was inserted perpendicularly into STN. The extracellular electrophysiological signals from nearby subthalamic neurons were amplified, filtered, converted through a digital analog interface (Model 3500, AM-system, USA) and stored on a computer. STN electrophysiological activity is also displayed on an oscilloscope. The single-unit discharges of STN were sorted by a signal-to-noise ratio of 3:1 or higher and by configurations of the spikes. In general, we would record the baseline single-unit discharges for 5 minutes, then record for another 5 minutes during microinjection of pharmacological agents (injection rate: 0.2  $\mu$ l/min), and then record for 5 minutes after cessation of the injection. Alternatively, in the experiments using the microdialysis probe membrane, six recording tungsten electrodes (0.002 inch in diameter, California Fine Wire) with a connector were bounded with a microdialysis cannula (AG-12, Eicom, Japan) for drug application. The distance between the recording sites and the microdialysis probe membrane (membrane length, 0.5 mm) was less than 500  $\mu$ m (e.g. 100). Pharmacological agents were continuously infused through the probe at a rate of 1  $\mu$ l/min. Drug concentrations ~10 times higher than that in the case with direct microinfusion were applied because typically only ~10% of the drug concentration would exist in the extracellular medium just outside the microdialysis membrane (e.g. 101).